Fibrils Formed in Vitro from α-Synuclein and Two Mutant Forms Linked to Parkinson's Disease are Typical Amyloid†

Kelly A. Conway, James D. Harper, and Peter T. Lansbury, Jr.*

Center for Neurologic Diseases, Brigham and Women's Hospital and Department of Neurology, Harvard Medical School, 77 Avenue Louis Pasteur, Boston, Massachusetts 02115

Received June 23, 1999; Revised Manuscript Received December 21, 1999

ABSTRACT: Two missense mutations in the gene encoding α-synuclein have been linked to rare, early-onset forms of Parkinson's disease (PD). These forms of PD, as well as the common idiopathic form, are characterized by the presence of cytoplasmic neuronal deposits, called Lewy bodies, in the affected region of the brain. Lewy bodies contain α-synuclein in a form that resembles fibrillar Aβ derived from Alzheimer's disease (AD) amyloid plaques. One of the mutant forms of α-synuclein (A53T) fibrillizes more rapidly in vitro than does the wild-type protein, suggesting that a correlation may exist between the rate of in vitro fibrillization and/or oligomerization and the progression of PD, analogous to the relationship between Aβ fibrillization in vitro and familial AD. In this paper, fibrils generated in vitro from α-synuclein, wild-type and both mutant forms, are shown to possess very similar features that are characteristic of amyloid fibrils, including a wound and predominantly unbranched morphology (demonstrated by atomic force and electron microscopies), distinctive dye-binding properties (Congo red and thioflavin T), and antiparallel β-sheet structure (Fourier transform infrared spectroscopy and circular dichroism spectroscopy). α-Synuclein fibrils are relatively resistant to proteolysis, a property shared by fibrillar Aβ and the disease-associated fibrillar form of the prion protein. These data suggest that PD, like AD, is a brain amyloid disease that, unlike AD, is characterized by cytoplasmic amyloid (Lewy bodies). In addition to amyloid fibrils, a small oligomeric form of α-synuclein, which may be analogous to the Aβ protofibril, was observed prior to the appearance of fibrils. This species or a related one, rather than the fibril itself, may be responsible for neuronal death.

Lewy bodies (LB's)[1] are intraneuronal cytoplasmic inclusions, often spherical and lamellar in appearance, that are characteristic of several neurodegenerative diseases, including diffuse Lewy body disease (DLBD), a dementia characterized by cognitive loss (*1*), and Parkinson's disease (PD), a movement disorder characterized by bradykinesia (difficulty in initiating movements) (*2, 3*). The role of LB's in the PD pathogenic process is unclear. Although considered to be a diagnostic marker of PD, Lewy bodies occur in neurons that appear to be among the healthiest (by morphological criteria) of those remaining in a Parkinsonian substantia nigra (when PD becomes clinically apparent, ca. 70% of nigral dopaminergic neurons have already been lost) (*2*−*5*). Thus, it is possible that Lewy bodies represent a successful strategy for neurons to sequester/deactivate a neurotoxic species (similar to the way that *Escherichia coli* deal with recombinant protein overexpression by inclusion body formation). Significantly, incidental, or asymptomatic, Lewy body disease has an approximately 10-fold greater prevalence than PD in the aged population (*6*). Whether the incidental Lewy body disease population is destined to develop clinical PD, or whether they represent a portion of the population that is able to sequester a toxic species in the form of LB's has not been determined.

Recently, families afflicted with an autosomal dominant early-onset form of PD have been found to harbor one of two point mutations (A53T, A30P) in the gene encoding the protein α-synuclein (*7, 8*). Although these mutations seem to be quite rare, they nevertheless may provide clues to the underlying pathogenesis of PD, since the early-onset form is identical in all other respects to idiopathic PD. α-Synuclein has been identified as a component of Lewy bodies in idiopathic PD and DLBD brain by immunohistochemical (*9*) and, in the case of DLBD, biochemical methods (*10*). In addition, α-synuclein epitopes are associated with neuritic inclusions that are characteristic of multiple system atrophy (MSA) (*11*−*14*) and Hallervorden−Spatz disease (HSD) (*12*). Finally, fibrils extracted and partially purified from DLBD brain were shown by immunogold electron microscopy to contain α-synuclein (*14*).

A portion of α-synuclein (residues 61−95) known as the non-Aβ component of plaque (NAC) was identified as a

† Supported in part by grants from the National Institutes of Health (AG08470 and AG14366).

* To whom correspondence should be addressed. Telephone: (617) 525-5260. Fax: (617) 525-5252. E-mail: lansbury@cnd.bwh.harvard.edu.

[1] Abbreviations: AD, Alzheimer's disease; AFM, atomic force microscopy; WT, human wild-type α-synuclein; A53T, human A53T α-synuclein mutant; A30P, human A30P α-synuclein mutant; CD, circular dichroism spectroscopy; DLBD, diffuse Lewy body disease; EM, electron microscopy; FTD, frontotemporal dementia; FTIR, Fourier transform infrared spectroscopy; HD, Huntington's disease; IPTG, isopropyl β-D-thiogalactopyranoside; LB, Lewy body; MSA, multiple system atrophy; MW, molecular weight; NAC, non-Aβ component; NFT, neurofibrillary tangle; PAGE, polyacrylamide gel electrophoresis; PBS, phosphate-buffered saline; PD, Parkinson's disease; PK, proteinase K; PrP, prion protein; SDS, sodium dodecyl sulfate; TBS, tris-buffered saline; thio T, thioflavin T.

10.1021/bi991447r CCC: $19.00
Published on Web 02/18/2000

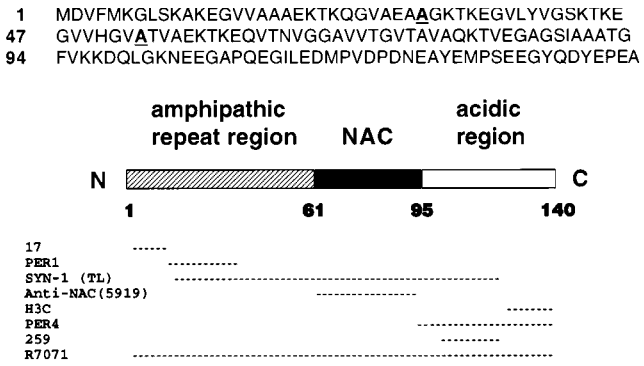

FIGURE 1: α-Synuclein sequence and epitope map. The two sites of early-onset PD-linked mutations (positions 30 and 53) are highlighted in the sequence at the top. At the bottom, epitopes and/or immunogens relevant to the antibodies utilized herein are mapped in the schematic sequence.

component of the insoluble fraction of AD brain homogenate (*15*). However, it has not been determined conclusively whether α-synuclein (previously also known as NACP) or NAC is an intrinsic component of the plaque-derived amyloid fibrils or plaque-associated dystrophic neurites, or whether NAC was derived from cosedimenting Lewy bodies (by proteolysis of α-synuclein?) often found in AD brain. Regardless, there is an intriguing parallel between early-onset forms of AD and PD. Both are characterized by fibrillar protein deposits (Aβ plaques in AD and α-synuclein LB's in PD) and are linked to autosomal dominant point mutations in genes that encode the fibril-forming proteins (*16*). Furthermore, the clinical overlap between AD and PD is far greater than would be predicted by random chance, consistent with a similar pathogenic process being involved in both diseases (*16*).

α-Synuclein is a 14 kD presynaptic protein of unknown function that is expressed at high levels in the brain (*17*−*21*). A role for α-synuclein in the learning process has been proposed, based on its elevated expression early in life (*22*), its presence in synapses (*17*, *23*), and its upregulation in zebra finch brain during song learning (*20*). α-Synuclein is a high-affinity inhibitor of phospholipase D, but the biological significance of this activity is unknown (*24*). The α-synuclein primary sequence can be divided into three regions (see Figure 1): (1) the amino terminal region (approximately residues 1−60, including the sites of both PD mutations) contains an 11 amino acid repeat sequence with a highly conserved hexamer motif (KTKEGV) and is predicted to assume amphipathic helical structure at an anionic membrane surface; (2) the central region, comprising the highly amyloidogenic NAC sequence (61−95) (*15*, *25*); (3) the carboxy terminal region (96−140), which is enriched in acidic residues (Glu and Asp) and in proline, suggesting that it adopts a disordered conformation (deletions from this region predispose α-synuclein toward fibrillogenesis (*26*)). Conformational studies of synthetic peptides based on each of these three regions support these predictions (*27*). Full-length α-synuclein is disordered ("random coil") in dilute solution; that is, it does not assume a stable globular structure as is typical for a protein of 140 amino acids (*27*). However, in association with lipid micelles (*27*, *28*), helical structure is stabilized, probably in the amino-terminal domain (*27*). This putative helical structure could be responsible for the weak association of α-synuclein with synaptic vesicles (*29*).

We and others have demonstrated that recombinant α-synuclein forms fibrils in vitro that resemble brain-derived material (*30*−*34*). Fibril formation by A53T is clearly accelerated relative to both WT and A30P (*30*). A30P does not fibrillize unusually rapidly, but, relative to WT, more rapidly forms apparently spherical oligomers with dimensions similar to Aβ protofibrils (diameter ca. 4 nm), intermediates in Aβ amyloid fibril formation (*35*−*38*). Two complementary assays, one that measures the loss of α-synuclein from solution (*34*) and another, the appearance of α-synuclein in a sedimentable fraction (*33*), confirm that A53T aggregates more rapidly than A30P and WT; one of these also reports that A30P is lost from solution more rapidly than is WT (although the morphology of the sedimented material was not investigated) (*34*).

To describe the α-synuclein aggregation/fibrillization process in more detail and to test a possible analogy between PD and AD, we analyzed α-synuclein fibrils formed in vitro using a combination of methods that have been used to study amyloid fibrils comprising Aβ and other proteins (*39*, *40*). These include electron microscopy (EM) and atomic force microscopy (AFM) to assess fibril morphology, Fourier transform infrared spectroscopy (FTIR) and circular dichroism spectroscopy (CD) to elucidate the constituent secondary structure, and binding of the amyloid histological dyes Congo red and thioflavin T (thio T), as well as protease sensitivity, to correlate species formed in vitro with material found in diseased tissue. We report herein that α-synuclein forms antiparallel β-sheet containing fibrils, with a similar morphology to those comprising other amyloid proteins. In contrast to the α-synuclein soluble monomer, fibrillar α-synuclein is protease-resistant, a trait commonly associated with the disease-associated form of the prion protein (PrP^{Sc}) (*41*), but also observed for Aβ amyloid fibrils (*42*). On the basis of the data reported herein, α-synuclein should be added to the growing list of amyloidogenic proteins and PD, DLBD, and MSA to the list of neurodegenerative amyloid diseases. Furthermore, Lewy bodies can be considered to be cytoplasmic amyloid.

MATERIALS AND METHODS

Recombinant α-Synuclein Expression and Purification. The pRK172/α-synuclein WT plasmid containing cDNA encoding WT human α-synuclein (provided by R. Jakes and M. Goedert, MRC Cambridge) was mutagenized using the QuikChange site-directed mutagenesis protocol (Stratagene). To create plasmid pRK172/α-synuclein A53T, a G to A mutation was introduced into the plasmid at nucleotide 157 and to create plasmid pRK172/α-synuclein A30P, a G to C mutation was introduced into the plasmid at nucleotide 88. Mutagenesis was verified by ABI 377 Fluorescent DNA sequencing. BL21(DE3) *E. coli* were transfected with pRK172/α-synuclein plasmids, and expression was induced by the addition of isopropyl β-D-thiogalactopyranoside (IPTG). Cells were harvested, resuspended in 10 mM Tris, pH 8, 1 mM EDTA, 1 mM PMSF (1/10 culture volume), and lysed by freezing in liquid nitrogen followed by thawing and probe sonication. Lysate was enriched for α-synuclein in two sequential ammonium sulfate precipitations, an initial ammonium sulfate precipitation (30% saturation at 0 °C) in which α-synuclein remains in the supernatant followed by a second ammonium sulfate precipitation (50% saturation

at 0 °C) in which α-synuclein was precipitated. The pellet was resuspended, loaded onto a ProteinPak DEAE 5PW column (21 × 150 mm, Waters) in 10 mM Tris, pH 7.4, and eluted in a gradient of 0−700 mM NaCl over 70 min. WT eluted at approximately 300 mM NaCl. Fractions containing α-synuclein (analyzed by Coomassie-stained SDS-PAGE) were concentrated in an Ultrafree-15, 5K MWCO filter (Millipore), loaded onto a Sephacryl S-300 2.6 × 30 cm size exclusion column (Pharmacia) and eluted in 100 mM NH_4HCO_3. α-Synuclein-containing fractions, identified by Coomassie-stained SDS-PAGE, were combined and lyophilized. All proteins were determined to be ca. 95% pure by SDS-PAGE and electrospray mass spectrometry (parent ions listed below). Amino acid composition was verified by amino acid analysis. WT amino acid analysis: Asx 9.3 (9), Thr 8.1 (10), Ser 2.7 (4), Glx 26.4 (24), Pro 4.5 (5), Gly 18.6 (18), Ala 19.0 (19), Val 18.4 (19), Met 4.4 (4), Ile 2.1 (2), Leu 4.4 (4), Tyr 3.5 (4), Phe 1.3 (2), His 1.1 (1), and Lys 15.6 (15); experimental MW (calcd MW) = 14 460 (14 460.2). A53T amino acid analysis: Asx 9.3 (9), Thr 9.0 (11), Ser 3.0 (4), Glx 27.0 (24), Pro 5.0 (5), Gly 18.3 (18), Ala 18.0 (18), Val 18.7 (19), Met 1.6 (4), Ile 2.0 (2), Leu 4.1 (4), Tyr 2.9 (4), Phe 2.0 (2), His 1.0 (1), and Lys 14.8 (15); MW = 14 490 (14 490.2). A30P amino acid analysis: Asx 9.4 (9), Thr 8.0 (10), Ser 2.9 (4), Glx 28.2 (24), Pro 5.6 (6), Gly 18.7 (18), Ala 18.1 (18), Val 18.2 (19), Met 3.9 (4), Ile 2.1 (2), Leu 4.5 (4), Tyr 3.8 (4), Phe 2.1 (2), His 1.2 (1), and Lys 14.7 (15); MW = 14 485 (14 486.2).

Preparation of α-Synuclein Incubations for Aggregation/Fibrillization Studies. Samples were dissolved in 10 mM phosphate buffer, 2.7 mM KCl, 137 mM NaCl, pH 7.4 (PBS) and, in some cases, filtered through a Millipore Microcon 100 K MWCO filter. Protein concentrations in the filtrate/incubation were determined by quantitative amino acid analysis. Samples were incubated at 37 °C without agitation. To ensure that no protein degradation was occurring during the prolonged incubations required to produce fibrils, both the supernatant and the pellet (after solubilization in 6 M guanidinium chloride) were analyzed when fibrils were removed. No significant degradation (to the extent of ≥5%) could be detected by SDS-PAGE/Western blot; both fractions appeared to be identical. In addition, electrospray mass spectrometric analysis of the solubilized (6 M guanidinium chloride) pellet showed a major parent ion corresponding to the full-length α-synuclein and a minor peak corresponding to hydrolysis at the notoriously acid-sensitive Asp-Pro amide (positions 119−120), which was estimated to be ≤5% by western blot.

Atomic Force Microscopy. At given time points, the aggregation incubations were mixed by gentle tapping and 2 μL was placed onto a surface of freshly cleaved mica. After incubating for 30 s (at room temperature), the substrate was rinsed twice with 50 μL water to remove salt and loosely bound peptide. Excess water was removed with a gentle stream of filtered compressed air, and the sample was imaged immediately. All images were obtained in ambient conditions in tapping mode using a Nanoscope IIIa force microscope (Digital Instruments, Santa Barbara, CA) operating in TappingMode with an etched silicon Nano Probe (model FESP: 125 μm cantilever, spring constant = 1−5 N/m, tip radius = 5−10 nm). Scanning parameters varied with individual tips and samples, but typical ranges were as follows: starting RMS amplitude, 0.6−1.2 V; setpoint, 0.4−1.0 V; resonant frequency, 60−80 kHz; scan rate, 0.8−2 Hz.

Electron Microscopy. An aliquot was removed from an α-synuclein aggregation incubation, diluted to 5 μM in H_2O, and adsorbed onto a Formvar-coated, carbon-stabilized copper grid (400 mesh). The grid was then rinsed briefly with H_2O, negatively stained with 2% aqueous uranyl acetate, air-dried, and examined with a JEOL 1200EX transmission electron microscope at an accelerating voltage of 80 kV.

Immuno-gold Electron Microscopy. An aliquot from an A53T aggregation incubation was diluted to an α-synuclein concentration of 5 μM and adsorbed onto Formvar-coated grids. The grids were rinsed briefly with TBS and blocked with 1% egg albumin. The grid was then incubated with the primary antibody (polyclonal PER1 at 1:50 dilution or polyclonal antibody PER4 at 1:1600 (*47*)), washed in TBS, and incubated again in colloid gold-conjugated goat anti-mouse IgG or goat anti-rabbit IgG secondary antibody. Control grids were incubated with secondary antibody alone. After a brief fixation with glutaraldehyde and a rinse with buffer, the grids were negatively stained with uranyl acetate, air-dried, and examined with a JEOL 100 CXII transmission electron microscope.

Circular Dichroism Spectroscopy (CD). An aliquot from a ca. 100 μM aggregation incubation was analyzed on an Aviv 62A DS spectrophotometer using a 0.02 cm cuvette at 25 °C.

Fourier Transform Infrared Spectroscopy (FTIR). α-Synuclein incubations were centrifuged at 14000*g* for 5 min to sediment fibrils. The supernatants were removed and the pellets were rinsed twice with H_2O to remove residual nonfibrillar adsorbed α-synuclein. Pelleted fibrils were resuspended in 100 μL H_2O and spread on a CaF_2 plate. The plate was dried in vacuo to remove excess H_2O. Infrared spectra were recorded on a Perkin-Elmer 1600 series FTIR spectrophotometer. Deconvolution was accomplished by Perkin-Elmer software and was based on bandwidth deconvolution.

Congo Red Birefringence. A 10 μL aliquot of a 300 μM α-synuclein suspension containing fibrils (confirmed by EM) was added to 10 μL of a 1% aqueous Congo red solution. The mixture was placed on a slide and covered with a coverslip. Birefringence was determined with an Olympus BX50 light microscope equipped with a polarizing stage.

Congo Red Binding. The concentration of Congo red was determined by absorption at 498 nm (extinction coefficient = 3.7×10^4 M^{-1}). A 100 μM stock solution of Congo red in PBS (pH 7.4) was prepared and filtered through a 0.2 μm cellulose acetate filter. Fibrillar α-synuclein (10 μM) was mixed with shaking in 2.5 μM Congo red in PBS, pH 7.4, at room temperature for 30 min. UV−vis absorption data were collected with a Hewlett-Packard HP8452A UV/VIS spectrophotometer in a 1 cm path length glass cuvette, recording absorption from 400 to 600 nm.

Thioflavin T Binding. A 100 μM aqueous stock solution of thio T was prepared and filtered before use through a 0.2 μm cellulose acetate filter. A 100 μL aliquot of this stock solution was added to a 1.9 mL suspension/solution (final [thio T] = 5 μM) containing between 0 and 250 nM α-synuclein (aliquots from incubations were first diluted ca. 20-fold to 10 μM in H_2O, then further diluted to ca. 1.9 mL with buffer) in 50 mM glycine-NaOH, pH 8.5. After 1 min,

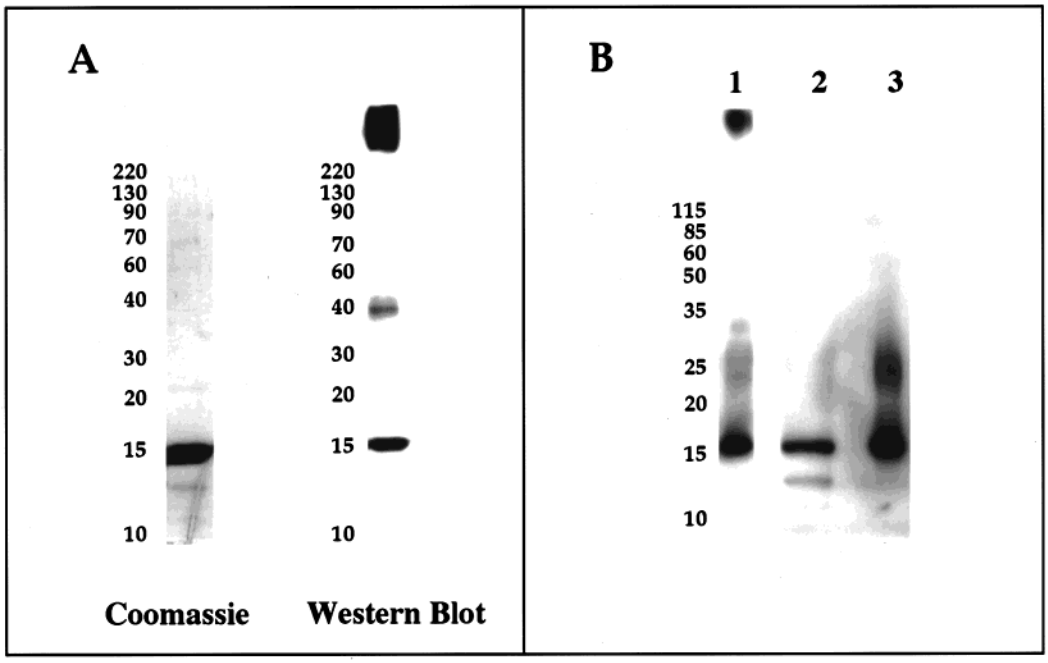

FIGURE 2: Analysis of recombinant α-synuclein by SDS-PAGE. Protein for these gels was filtered through a 0.2 μm filter as a final step. All three variants (WT, A53T, and A30P) were indistinguishable with respect to SDS-PAGE; representative gels are shown. (Panel A) High molecular weight bands of A30P were detected by western blot with polyclonal α-synuclein antibody R7071 (raised to recombinant α-synuclein WT) but not by Coomassie R-250 staining. Filtration of α-synuclein through a 100 kD MW-cutoff filter successfully removed the high molecular weight species that did not enter the gel, but not the ca. 35 kD species. However, this band often reformed during prolonged incubations. (Panel B) High molecular weight bands of A53T (lane 1), detected by western blot with monoclonal α-synuclein antibody SYN-1, were abolished by treatment with 85% formic acid (lane 2) or 6 M guanidinium chloride (lane 3). The truncated band in lane 2 arises from acidic hydrolysis of α-synuclein, possibly at the D119−P120 amide bond (a parent ion corresponding to this fragment was detected by electrospray mass spectrometry). The identities of the bands at ca. 25 kD (lanes 1 and 3) are under investigation.

fluorescence measurements were made with an SLM 8000C fluorescence spectrophotometer. Scans were performed in a 1 cm^2 fluorescence cuvette, exciting at 446 nm wavelength (slit width 4 nm). The fluorescence emission spectrum was recorded from 450 to 600 nm (slit width 16 nm). Measurements were obtained with a 1 s integration.

Proteinase K Digestion. A 2 μL aliquot of 175 μg/μL Proteinase K (Boehringer Mannheim) was added to 5 μL of α-synuclein (100 μM) in PBS, pH 7.4. After a 1 h incubation at 37 °C, 1 μL of 10 mM Pefabloc SC (Boehringer Mannheim) in 10 mM sodium phosphate buffer, pH 7.4, was added to stop proteolysis. Proteolyzed α-synuclein was separated on a 10−20% Tricine polyacrylamide gel, which was developed with silver stain to visualize all proteins. Immunoreactivity of crude digestion products was determined by dot-blotting.

RESULTS

Expression of Recombinant WT, A53T, and A30P. The pRK172/α-synuclein WT plasmid was altered to contain the PD point mutations, and mutant proteins were purified according to a slight modification of a published procedure (*27*). All proteins (WT, A53T, and A30P) were estimated to be 90−95% pure by Coomassie R-250 denaturing polyacrylamide gel (Figure 2, panel A), amino acid analysis, and electrospray mass spectroscopy. The expression and purification scales were increased ca. 10-fold from our previous work (*27*) to produce in excess of 100 mg α-synuclein per 4 L culture (yields determined by amino acid analysis). Analysis of all three forms of recombinant α-synuclein by denaturing gel electrophoresis revealed a discrepancy between the pattern of bands, depending on the method of protein detection (WT, A53T, and A30P were indistinguishable, see Figure 2). Staining with Coomassie blue or silver nitrate, which are nonspecific methods, indicated that ca. 95% of the total α-synuclein migrated as a monomer of 15 kD. However, Western blotting with four antibodies specific to α-synuclein (antibodies R7071, raised to full-length recombinant WT (data shown in Figure 2), H3C (courtesy of D. Clayton and J. George, epitope α-synuclein 126−140), 259 (courtesy of T. Iwatsubo, immunogen α-synuclein 104−119), and SYN-1 (Transduction Labs, immunogen WT 15−123)) indicated a significant level of two species of higher molecular weight, in addition to the α-synuclein monomer. We believe that both of these are α-synuclein oligomers, since they cross-react with four α-synuclein antibodies and are abolished by treatment with 6 M guanidinium chloride or formic acid (see Figure 2, panel B). Western blotting overestimates the amount of the high molecular weight bands, possibly due to the fact that a bivalent antibody will preferentially bind an oligomer with two accessible epitopes. The ca. 35 kD (possibly dimeric) species has been observed by other laboratories (*29*, *43*) and constitutes much less than 5% of total protein as detected by Coomassie. The high molecular weight band, which does not enter the gel, has also been observed by other laboratories (for example refs *31* and *44*) and can be removed by filtration through a 100 kD MW-cutoff filter, but passes through a 0.2 μm filter (Whatman). Removal of this band had no effect on any of the properties discussed herein, although the rate of fibrillization and β-sheet formation (Figure 5) was decreased. After

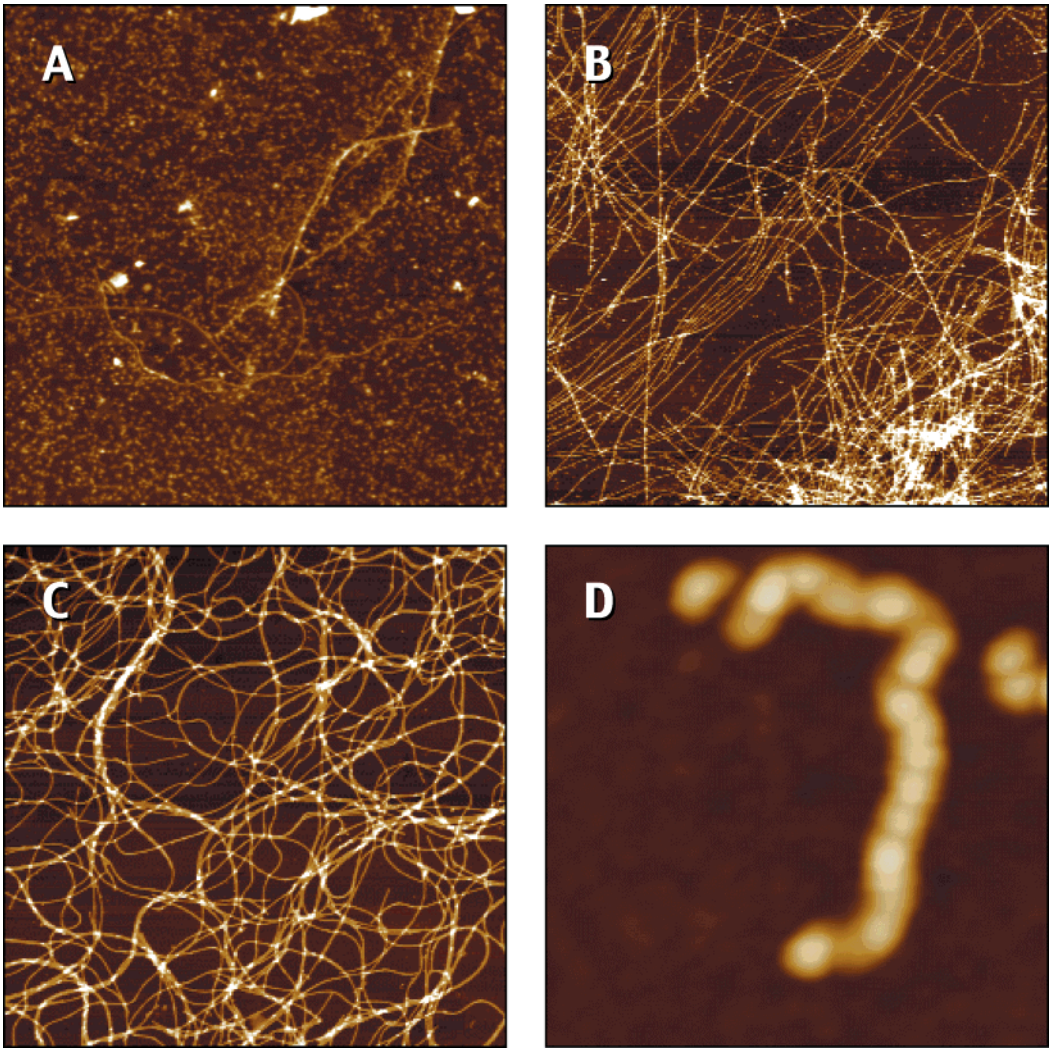

FIGURE 3: AFM analysis of α-synuclein fibrillization. (A) 300 μM WT after 4 months of incubation, (B) 100 μM A53T after 1 month, (C) 300 μM A30P after 4 months, and (D) 50 μM A30P after 4 months (This species may be an A30P protofibril). Panels A−C are 5 × 5 μm^2; Panel D is 250 × 250 nm^2.

its removal, the high molecular weight band was occasionally observed to reform during the course of fibrillization.

α-Synuclein Forms Typical Amyloid Fibrils as well as Additional Morphologies. As reported previously, incubations of WT, A53T, and A30P (100−300 μM protein in phosphate buffered saline, pH 7.4 at 37 °C) all gave rise to fibrils within 1−2 months (*30*). The fibrils were ca. 8−10 nm in height as measured by AFM (Figure 3) and approximately 10 nm in width as measured by EM (Figure 4). When fibrils were grown at higher α-synuclein concentration (300 vs 100 μM, as shown in Figure 4) two-filament twisted morphology was often observed, especially in fibrils comprising A53T (periodicities of 45, 65, and 95 nm). Individual filaments of ca. 5 nm in height and small, spherical species, ca. 4 nm in height, were also detected (AFM, EM) for all variants. In the case of A30P, a linear association/annealing of these spherical species, resembling an Aβ protofibril (length ca. 325 nm), was occasionally observed (Figure 3, panel D). While the dimensions of the individual α-synuclein fibrils produced in vitro were similar for WT and mutant proteins, a distinctly different morphology could be produced by solutions of A30P incubated at 300 μM as compared to WT and A53T at identical concentrations. A30P fibrils formed under these conditions reproducibly displayed polymorphic, sometimes almost sinusoidal, morphologies, reminiscent of bacterial flagellar filaments (Figure 3, panel C; Figure 4, panel C) (*45*), whereas the A53T and WT fibrils were predominantly straight (slight curvature detected in less than 1% of the fibrils comprising A53T (panel B in Figures 3 and 4) and WT (panel A in Figures 3 and 4)). In contrast, incubations at lower α-synuclein concentrations, e.g. 100 and 200 μM, produced similar straight fibrils for A30P, WT, and A53T (not shown). A dense fibrillar meshwork, reminiscent of the Lewy body core (*46*), was commonly observed (Figure 4, panel E). Bundles of fibrils, longer than 20 μm, were formed by all α-synuclein variants (Figure 4, panel D).

The Fibrils Formed in Vitro Resemble Those in Lewy Body-containing Brain. The measured dimensions (AFM) and observed morphologies of in vitro α-synuclein fibrils were comparable to the ca. 10 nm wide fibrils directly observed by EM of Lewy bodies in PD brain tissue sections (*6*). α-Synuclein-containing fibrils extracted from cortical Lewy bodies of diffuse Lewy body disease (DLBD) brain (*1, 47*) and from filamentous inclusions of multiple system atrophy (MSA) brain (*12, 14*) are also indistinguishable with respect to morphology and dimension. Some of these extracted fibrils are ca. 10 nm in width ("straight") and others have a "twisted appearance" (width varies between 5 and

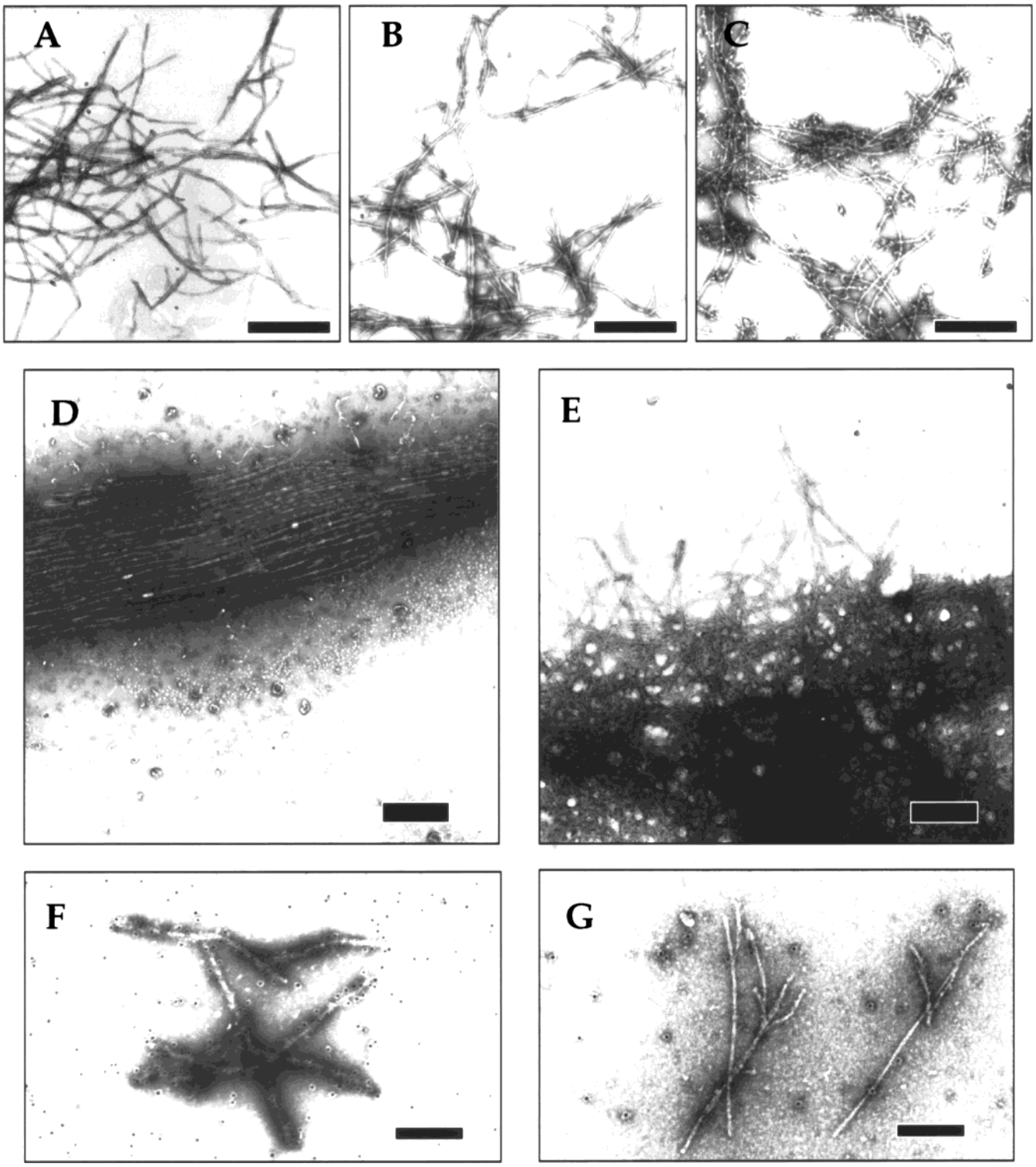

FIGURE 4: EM analysis and immunogold staining of α-synuclein fibrils. (A) 300 μM WT after 1 month, (B) 200 μM A53T after 1 month, (C) 300 μM A30P after 3 months, (D) 200 μM A53T after 2 weeks, (E) 200 μM WT after 1.5 months, (F) 200 μM A53T after 1 month, labeled with PER4 antibody, and (G) 200 μM A53T after 1 month, labeled with PER1 antibody. Scale bar = 500 nm in panels A−E, and 250 nm in panels F−G.

18 nm), possibly involving two subfilaments (*14, 47*). Filaments of 5 nm width, in isolation and projecting from fibril termini, are also observed in DLBD brain-derived samples (*47*).

Immunogold Electron Microscopy Reveals a Similarity between α-Synuclein Fibrils Produced in Vitro and Those Formed in Vivo and Subsequently Extracted from Postmortem Brain. The similarity of α-synuclein fibrils formed in vitro to those derived from diseased brain was tested using immunogold electron microscopy. A53T fibrils (and other assemblies) were treated with four antibody preparations that have been used to stain Lewy bodies in PD (*9, 10*) and DLBD brain tissue (*10, 47*) and cytoplasmic inclusions in MSA brain tissue (*12, 14*). These antibodies were (1) a polyclonal antibody raised against residues 1−10 of α-synuclein (17 from T. Iwatsubo)(*10*), (2) a monoclonal antibody

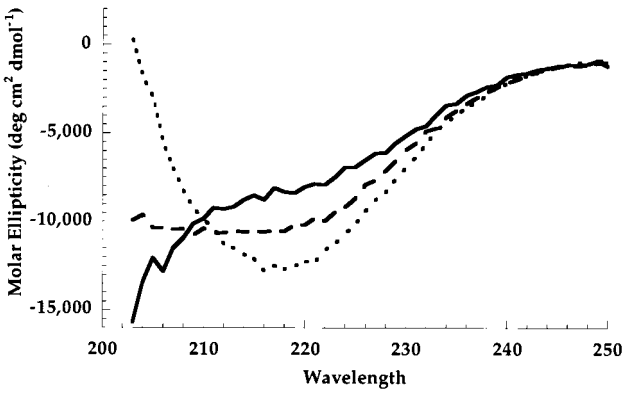

FIGURE 5: Detection of A53T β-sheet formation by CD. Spectrum of A53T was measured at various timepoints during 37 °C incubation ([A53T] = 100 μM). Day 0 (solid line), Day 3 (dashed line), and Day 7 (dotted line). This sample was filtered through a 0.2 μm filter as the final step of purification (SDS-PAGE similar to Figure 2). When the sample was filtered through a 100 kD MW-cutoff filter prior to incubation, a similar transition was observed; however, it took place much more slowly (data not shown).

(H3C from J. George and D. Clayton) that recognizes an epitope at the extreme C-terminus (residues 126−140) (*20*), (3) a polyclonal antibody (PER4 from M. Goedert) that recognizes an undefined epitope in the α-synuclein C-terminal domain (*47*), and (4) a polyclonal antibody (PER 1 from M. Goedert) that was raised against WT residues 11−34. As reported previously (*30*), antibody 17 labeled the sides of fibrillar A53T assemblies and nonfibrillar, spherical A53T oligomers, whereas H3C preferentially labeled the nonfibrillar oligomers (*30*). It has been reported (M. Goedert, personal communication) that H3C decorates the sides of LB-derived fibrils. This apparent discrepancy may only be the consequence of competitive binding; that is, the C-terminal epitope may be more accessible in the spherical species that are present in the material generated in vitro, but do not copurify with brain-derived fibrils. PER4, like 17, labeled A53T fibrils and spherical assemblies (Figure 4, panel F). PER4 decorates the sides of fibrils derived from DLBD brain (*47*). Finally, PER1 stained spherical A53T assemblies, but not α-synuclein fibrils produced in vitro (Figure 4, panel G). However, PER1 decorates one terminus, but not the sides of ex vivo DLBD fibrils, suggesting that the fibrils have a polarized structure and undergo unidirectional growth (*47*). Again, the discrepancy between in vitro and ex vivo material is more likely due to preferential binding of PER1 to A53T spheres (not present in extracted material), rather than to a structural difference between A53T fibrils formed in vitro and WT fibrils formed in vivo.

Circular Dichroism Spectroscopy Indicates that β-Sheet Structure is Formed Concurrently with Fibrillization. Incubations of α-synuclein were sampled at various times and analyzed by CD to study changes in average α-synuclein secondary structure during fibril formation. Freshly prepared solutions of α-synuclein in PBS generated a CD spectrum with a minimum at ca. 200 nm, characteristic of a protein that is primarily random coil (*27*). Upon incubation at 37 °C, the minimum at ca. 200 nm disappeared and was replaced by a characteristic β-sheet minimum at ca. 220 nm (Figure 5) (*48*). A similar transition from random coil to β-sheet is observed during the in vitro fibrillogenesis of Aβ40 (*49*). Scattering due to the presence of turbid, insoluble material is known to influence spectral intensity in experiments of this type, producing a redshifted, flattened CD spectra (*50*). However, the solutions analyzed in Figure 5 were not turbid. Furthermore, turbid α-synuclein solutions containing fibrillar material showed a loss of the "random coil" minimum at ca. 200 nm, but little or no appearance of a β-sheet minimum at ca.. 220 nm, as was seen in the nonturbid solutions (as expected, an inverse correlation between turbidity and the magnitude of the β-sheet minimum was seen). This coil-to-sheet transition was slowed when the suspension was initially filtered through 100 kD MW-cutoff filter prior to data acquisition. In addition, the rate of the transition was affected by the PD mutations (A53T was faster than WT and A30P (*51*)), consistent with fibril formation being responsible for the observed change. It is difficult to estimate, from CD spectra, the percentage of the total α-synuclein molecules and/or the percentage of the α-synuclein backbone that populate β-sheet structure (*48*). In agreement with the conclusion that CD spectra demonstrate conversion to β-sheet structure, α-synuclein fibrils, analyzed by Fourier transform infrared spectroscopy, exhibited an amide I band consistent with β-sheet and distinctly different than that of a random coil or α-helix (*40, 48, 52*).

α-Synuclein Fibrils Contain Antiparallel β-Sheet Structure as Detected by Fourier Transform Infrared Spectroscopy. Infrared spectroscopy of α-synuclein fibrils formed in vitro produced the characteristic amyloid fibril spectrum of an antiparallel β-sheet. No clear differences were detected between fibrils produced from WT (Figure 6, panel A) and mutant forms of α-synuclein (Figure 6, panels B and C). The predominant tertiary structure was confirmed by the co-occurrence of a high-intensity, low-frequency amide I absorption band at 1626 cm^{-1} and a low-intensity, high-frequency band at 1690 cm^{-1} (*40, 52*). These bands match well with the absorption bands of the known antiparallel β-sheet polypeptides polyglycine, β-polyalanine, poly(alanylglycine), and especially polyglutamate (*53*). The amide I absorption bands for β-polyglutamate occur at 1624 cm^{-1} (strong) and 1693 cm^{-1} (weak). The split amide I absorption band (typically split by 60−80 cm^{-1}) is a consequence of transition dipole coupling that only occurs when β-strands are oriented in an *antiparallel* fashion (*53*). The high-frequency absorption band thus distinguishes antiparallel from parallel β-sheet. The fact that this band was not detected in a previous study of fibrils comprising WT and mutant forms of α-synuclein may be due to the low sensitivity of the spectrometer employed and/or the data handling method (second derivative) (*34*). The absorption band at 1660 cm^{-1} (Figure 6) may be attributed to α-helix, random coil, β turn, or a combination of these structures. The presence of this band indicates that a portion of the α-synuclein sequence is not involved in the core antiparallel β-sheet structure of the fibril. Finally, the existence of some parallel β-sheet structure in the α-synuclein fibril is not ruled out.

Congo Red Exhibits an Absorption Shift and Birefringence Upon Binding to Fibrillar α-Synuclein. Fibrillar α-synuclein was tested for binding to the dye Congo red, which is commonly used to stain amyloid in tissue sections (*54*−*57*). Birefringence is observed for Aβ40 fibrils formed in vitro (Figure 7, panel B) (*58*) as well as for in vitro fibrils comprising insulin (*59*) and transthyretin (*60*). Similarly, Congo red bound to WT fibrils with yellow-green birefrin-

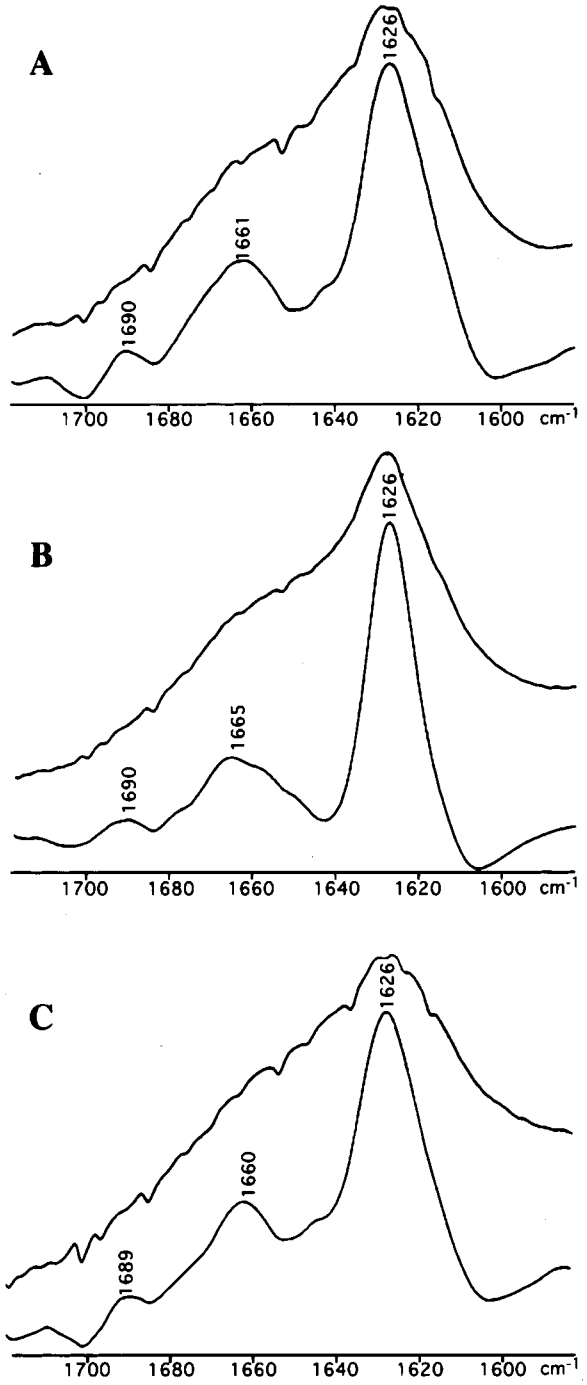

FIGURE 6: Detection of antiparallel β-sheet structure in α-synuclein fibrils by FTIR. The three variants gave practically indistinguishable spectra; WT (Panel A), A53T (Panel B), and A30P (Panel C). In each panel, the undeconvoluted spectrum appears at the top and the deconvoluted spectrum at the bottom.

gence, when observed under a polarizing microscope (Figure 7, panel A), a defining characteristic of ex vivo amyloid. The binding of Congo red to amyloid fibrils comprising insulin or Aβ40 has been demonstrated to shift its absorption spectrum to longer wavelengths (*58, 61*). Upon incubation with WT fibrils, the absorption spectrum of Congo red was similarly shifted from a λ_{max} of 490 nm in PBS (Figure 7, panel C) to a λ_{max} of 540 nm in the presence of fibrillar α-synuclein. An indistinguishable shift occurred upon binding of Congo red to fibrils prepared from A53T or A30P. No change was observed in the presence of soluble, monomeric α-synuclein (not shown).

Binding of Thioflavin T to Fibrils Enhances Its Fluorescence Emission Intensity at 490 nm. Thioflavin T is commonly used to stain amyloid in tissue sections and to detect amyloid fibrils in vitro (*56, 62*). Both soluble and fibrillar α-synuclein were analyzed for thio T binding in a fluorescence assay devised by Naiki et al. (*63*). Free thio T fluoresces weakly at 438 nm when excited at 350 nm (*63*). In the presence of amyloid fibrils, a strong thio T fluorescence emission is observed at 490 nm upon excitation at 450 nm. The emission is linear relative to the concentration of fibrils (Figure 8). This effect has been demonstrated with amyloid fibrils comprising insulin (*62*), human islet amyloid polypeptide (IAPP) (*64*), a peptide based on the human prion protein PrP 106−126 (*65*), Aβ140 (*62, 66*), and with tau paired helical filaments (*67*). Incubation of fibrillar α-synuclein (50 nM) with thioflavin T (5 μM) produced the characteristic effect (Figure 8). Fluorescence emission scans from 460 to 560 nm for monomeric, soluble α-synuclein (250 nM) incubated with thioflavin T were virtually identical to those of thioflavin T in the absence of added protein.

Fibrils Comprising α-Synuclein are Protease-resistant Relative to Soluble α-Synuclein. Amyloid formation has been shown to impart a partial resistance to proteolysis to the fibrillar protein relative to the soluble, monomeric protein (*41, 42, 68, 69*). The disease-associated development of protease-resistance in the prion protein is well-documented in the transmissible spongiform encephalopathies in which a protease resistant form of the prion protein (PrP^{sc}) that is resistant relative to the normal cellular protein (PrP^{c}) is characteristic of the diseased brain (*68, 70, 71*). The α-synuclein fibrils produced in vitro behaved like typical amyloid fibrils in this regard. Whereas treatment of monomeric A53T with proteinase K (PK) for 1 h resulted in almost complete digestion of A53T, treatment of fibrillar A53T generated a distinct protease-resistant band that migrated more rapidly than the 10 kD molecular weight marker (Figure 9). The distinct protease-resistant band may correspond to the sequence protected in the amyloid fibril core. The protease-resistant material in digested fibrillar A53T reacted with the polyclonal antibody R5919 (raised to NAC) and with SYN-1 monoclonal antibody (Transduction Labs; immunogen is rat WT residues 15−123) and was not labeled by the N-terminal antibody 17 (raised to α-synuclein residues 1−10) nor by the C-terminal antibody H3C (epitope is canary α-synuclein residues 126−140) (dot blot studies are not shown). Attempts to identify the protease-resistant band are underway. Fibrils comprising WT and A30P also demonstrated protease-resistance.

DISCUSSION

α-Synuclein Fibrils Formed in Vitro, as well as Those Extracted from Postmortem Brain, Have all of the Characteristics that are Classically Associated with Amyloid Fibrils. Amyloid is a generic term that has taken on a specific meaning pertaining to Alzheimer's disease plaques and their constituent fibrils. However, the term was originally coined to reflect unusual tinctatorial properties of the material, which suggested a carbohydrate composition. More recently, amyloid has been shown to be proteinaceous and fibrillar and has been associated with many constituent proteins and many diseases (*39*). Amyloid fibrils are rigid, unbranched, and approximately 10 nm wide. When stained with Congo red

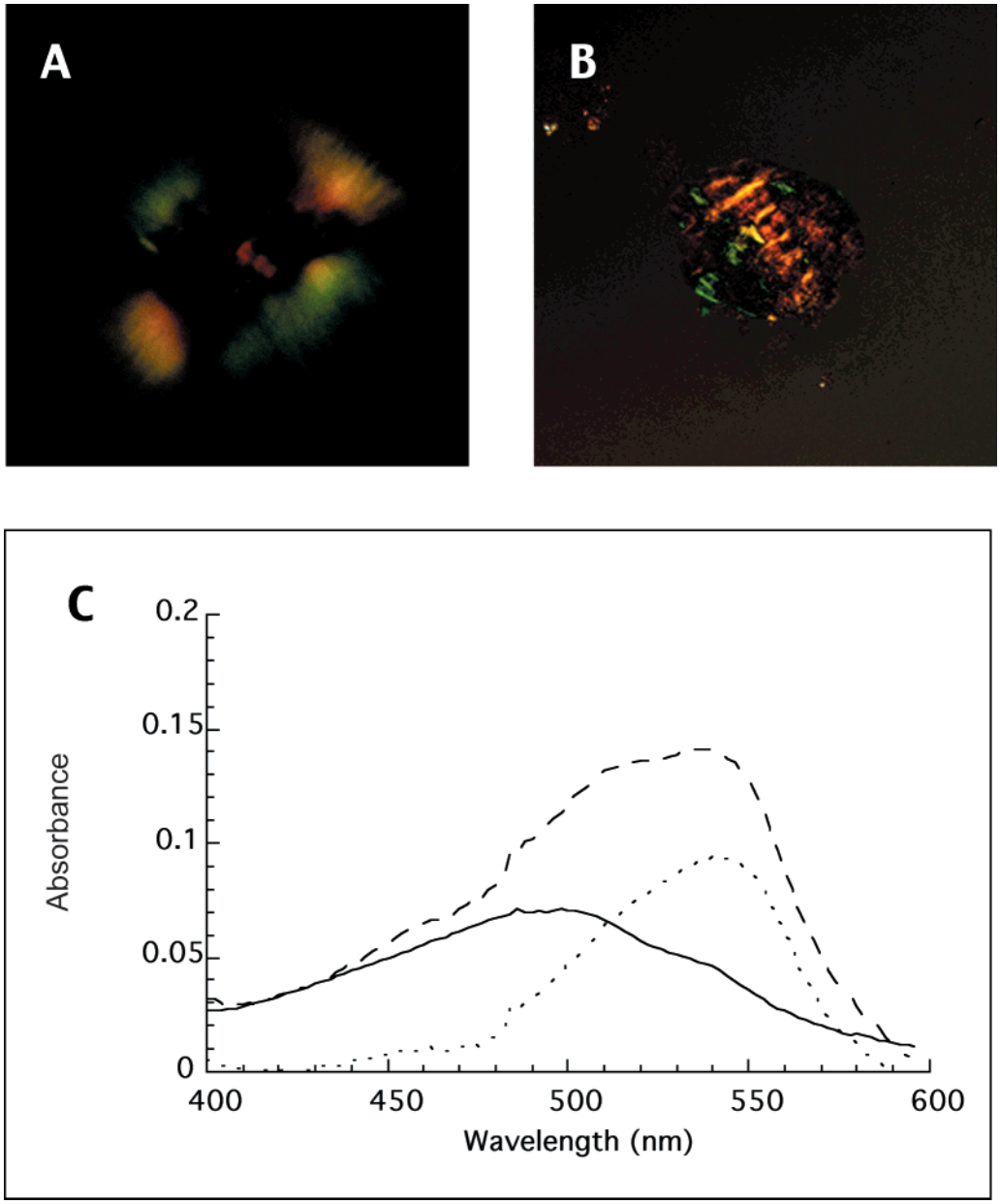

FIGURE 7: α-Synuclein WT fibrils bind to Congo red in an "amyloid-like" manner. Panels A and B show birefringent staining observed through a polarized filter: (A) WT fibrils, (B) Aβ40 amyloid fibrils. (C) Congo red binding to WT fibrils shifts the absorbance spectra of Congo red: Congo red (solid line); Congo red incubated with α-synuclein fibrils, corrected for scatter due to fibrils (dashed line); the difference spectrum (dotted line), which shows the shifted spectrum of bound Congo red.

and observed under a polarizing light microscope, amyloid fibrils exhibit "apple green" birefringence. In addition, amyloid fibrils typically bind thioflavin T, resulting in a specific fluorescence enhancement. Amyloid fibrils contain significant amounts of antiparallel β-sheet structure, most easily detected by FTIR (*40*, *72*) and are typically resistant to proteolysis as compared to the constituent proteins in soluble monomeric form.

α-Synuclein fibrils, formed in vitro from recombinant proteins, demonstrated each of these properties. The fibrils were measured to be 8−10 nm in width by EM and ca. 10 nm in height by AFM (*30*) and appeared to be constructed by the winding of two 4−5 nm filaments (*26*, *30*). The fibrils produced FTIR and CD spectra that are characteristic of antiparallel β-sheet structure. Birefringent staining with Congo red (*55*, *73*, *74*) was observed and characteristic shifts in the absorption and fluorescence spectra of fibril-bound

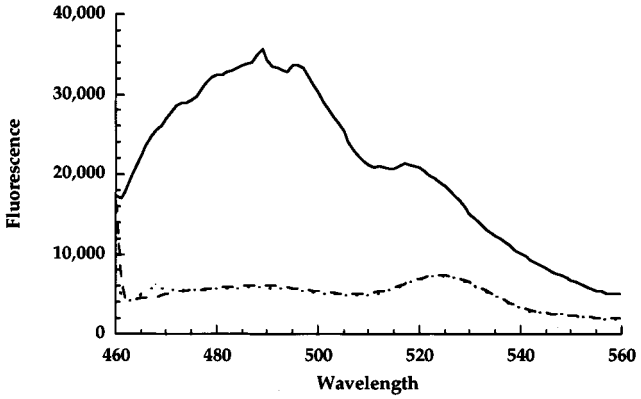

FIGURE 8: α-Synuclein WT fibrils bind to thioflavin T, enhancing its fluorescence emission. H_2O blank (dotted line); soluble WT at 250 nM (dashed line); and fibrillar WT at 50 nM (solid line). Excitation at 446 nm.

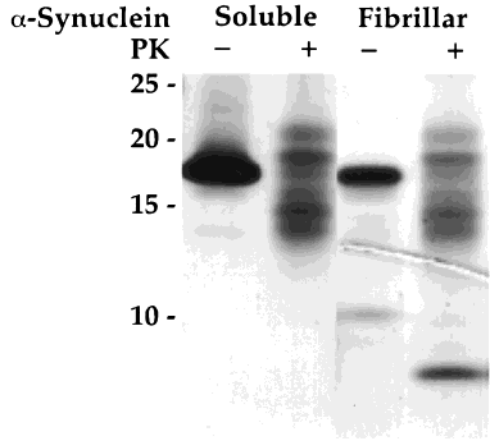

FIGURE 9: Fibrillar A53T demonstrates increased resistance to digestion with proteinase K. PK-treated samples were separated on a 10−20% tricine polyacrylamide gel, which was developed with silver stain. Soluble α-synuclein A53T, migrating at ca. 17 kD, was completely degraded after PK treatment (group of bands from 15 to 20 kD in a PK-treated sample is derived from the commercial PK; the intensity of these bands increases with the amount of added PK). Treatment of fibrillar A53T with PK generates a distinct band running faster than the 10 kD marker. The identity of the α-synuclein-derived fragment has not been determined. Fibrils comprising WT and A30P also demonstrated striking protease resistance.

Congo red and thioflavin T, respectively, were measured. Finally, the α-synuclein fibrils were unusually protease-resistant. Although the segment of primary sequence that constitutes the protease-resistant core has not been identified, it was shown to contain the central NAC sequence, but not epitopes at the N- and C-termini. These observations support the proposal, suggested by immunogold staining of Lewy body-derived α-synuclein fibrils, that truncation of α-synuclein is not necessarily responsible for its fibrillization in PD, DLBD, or MSA, although truncation can clearly accelerate in vitro fibrillization (*26*).

PD-linked α-Synuclein Mutations Cause Minor Perturbations in Fibril Structure and Morphology. Fibril widths and morphologies were similar for WT and the two mutant proteins, although A30P at high concentration formed an unusual curved morphology that had not been reported previously, possibly due to the practice, in other laboratories, of stirring the protein to hasten its aggregation (*33, 34*). No clear difference in secondary or tertiary structure that could explain the significant differences with respect to rates of fibril formation (*30*) seemed to be induced by PD-linked mutations. This is not to say, for example, that WT could seed fibrillization of A53T or vice versa. In fact, that issue and the possible formation of fibrils containing two α-synuclein variants (e.g., WT and A53T) are under investigation.

α-Synuclein Forms Spherical and Elongated Oligomers of Half the Fibril Height under in Vitro Conditions Where Fibril Formation Is Observed: Are These Protofibrils? Spherical species, ca. 4 nm in height, were formed by all three α-synuclein variants (*30*). In the case of A30P, elongated 4 nm high species were observed before the detection of fibrils. The possible intermediacy of these species is suggested by the morphological similarities between α-synuclein fibrillization and Aβ fibrillization. Fibrillization of Aβ has been demonstrated to proceed via a protofibril intermediate (*35, 37, 38, 75*).

Are Neuronal Cytoplasmic Amyloidoses a New Class of Neurodegenerative Disease? Although most systemic amyloid diseases are characterized by extracellular amyloid plaques, the work presented herein suggests that Lewy bodies may be cytoplasmic amyloid deposits. It is important to note that the cytoplasmic protein tau, the primary constituent of neurofibrillary tangles (NFT's) that are characteristic of AD and frontotemporal dementia (FTD) (*76*), like α-synuclein, forms fibrils in vitro that have some characteristics of amyloid (thio T fluorescence enhancement, morphology, nucleation-dependent assembly) (*67, 77*). Thus, NFT's may also fit the definition of amyloid. It is striking that PD, DLBD, FTD, and AD are characterized by cytoplasmic fibrillar inclusions, either Lewy bodies or NFT's, but only AD is characterized by extracellular plaques. It is possible to envision many cytoplasmic events that could create local concentrations in excess of the critical concentration (for example, binding to lipid surfaces (*27−29*) or molecular crowding (*78*) any of which could be linked to disease). It is important to emphasize that disease-associated intraneuronal fibrillar inclusions are not necessarily cytoplasmic; Huntington's disease (HD) is characterized by nuclear inclusions comprising the protein huntingtin (Htn). The constituent fibrils resemble amyloid fibrils formed in vitro from a Htn fragment (*79*). However, the role of these nuclear inclusions in HD pathogenesis has not been determined (*80, 81*).

Is the α-Synuclein Amyloid Fibril, a Prefibrillar Intermediate, or an Alternative α-Synuclein Oligomer that Forms during Fibrillization Responsible for Neurodegeneration? The work reported herein is focused on the fibrillar qualities of α-synuclein, since α-synuclein fibrils, in the form of Lewy bodies, are associated with postmortem PD brain, and the PD-linked α-synuclein A53T mutation promotes the formation of fibrils in vitro. However, it is possible that the fibrils themselves are inert and that formation of the pathogenic species is merely linked to fibrillization. In fact, one could argue that once fibrillization is allowed to proceed unchecked, fibril formation may be protective, sequestering toxic, α-synuclein-derived oligomeric species (*3−5*). Biophysical considerations argue that a partially folded intermediate with a high surface area-to-volume ratio, perhaps a protofibril, could be more toxic that the product fibril (*82*). According to this proposal, factors that favor fibrillogenesis may actually protect against PD by preventing the accumulation of a prefibrillar toxic species. Conversely, factors that slow a putative protofibril-to-fibril conversion could accelerate disease onset and progression by causing accumulation of a toxic intermediate. Drug candidates that are selected because they are α-synuclein fibril inhibitors may fall into this latter category and could, therefore, actually accelerate disease progression, an effect opposite to the desired one.

ACKNOWLEDGMENT

We thank Cynthia Lemere, Matthew Goldberg, Dominic Walsh and Y. Xu for assistance in performing selected experiments.

SUPPORTING INFORMATION AVAILABLE

Western blot analysis of WT, A53T, and A30P α-synuclein after fibril disaggregation. This information is available free of charge via the Internet at http://pubs.acs.org.

REFERENCES

1. Kosaka, K., and Iseki, E. (1996) *Curr. Opin. Neurol. 9*, 271−5.
2. Pollanen, M. S., Dickson, D. W., and Bergeron, C. (1993) *J. Neuropath. Exp. Neurol. 52*, 183−191.
3. Forno, L. S. (1996) *J. Neuropathol. Exp. Neurol. 55*, 259−72.
4. Tompkins, M. M., Basgall, E. J., Zamrini, E., and Hill, W. D. (1997) *Am. J. Pathol. 150*, 119−31.
5. Tompkins, M. M., and Hill, W. D. (1997) *Brain Res. 775*, 24−9.
6. Forno, L. S., and Langston, J. W. (1993) *Neurodegen. 2*, 19−24.
7. Polymeropoulos, M. H., Lavedan, C., Leroy, E., Ide, S. E., Dehejia, A., Dutra, A., Pike, B., Root, H., Rubenstein, J., Boyer, R., Stenroos, E. S., Chandradekharappa, S., Athanassiadou, A., Papapetropoulos, T., Johnson, W. G., Lazzarini, A. M., Duvoisin, R. C., Di Iorio, G., Golbe, L. I., and Nussbaum, R. L. (1997) *Science 276*, 2045−2047.
8. Kruger, R., Kuhn, W., Muller, T., Woitalla, D., Graeber, M., Kosel, S., Przuntek, H., Epplen, J. T., Schols, L., and Riess, O. (1998) *Nat. Genet. 18*, 106−108.
9. Spillantini, M. G., Schmidt, M. L., Lee, V. M.-Y., Trojanowski, J. Q., Jakes, R., and Goedert, M. (1997) *Nature 388*, 839−840.
10. Baba, M., Nakajo, S., Pang-Hsien, T., Tomita, T., Nakaya, K., Lee, V. M.-Y., Trojanowski, J. Q., and Iwatsubo, T. (1998) *Am. J. Pathol 152*, 879−884.
11. Arima, K., Ueda, K., Sunohara, N., Arakawa, K., Hirai, S., Nakamura, M., Tonozuka-Uehara, H., and Kawai, M. (1998) *Acta Neuropathol. (Berl) 96*, 439−44.
12. Tu, P.-H., Galvin, J. E., Baba, M., Giasson, B., Tomita, T., Leight, S., Nakajo, S., Iwatsubo, T., Trojanowski, J. Q., and Lee, V. M.-Y. (1998) *Ann. Neurol. 44*, 415−422.
13. Wakabayashi, K., Yoshimoto, M., Tsuji, S., and Takahashi, H. (1998) *Neurosci. Lett. 249*, 180−2.
14. Spillantini, M. G., Crowther, R. A., Jakes, R., Cairns, N. J., Lantos, P. L., and Goedert, M. (1998) *Neurosci. Lett. 251*, 205−8.
15. Ueda, K., Fukushima, H., Masliah, E., Xia, Y., Iwai, A., Yoshimoto, M., Otero, D. A. C., Kondo, J., Ihara, Y., and Saitoh, T. (1993) *Proc. Natl. Acad. Sci. U.S.A 90*, 11282−11286.
16. Lansbury, P. T. (1997) *Neuron 19*, 1151−1154.
17. Maroteaux, L., Campanelli, J. T., and Scheller, R.H. (1988) *J. Neurosci. 8*, 2804−2815.
18. Maroteaux, L., and Scheller, R.H. (1991) *Mol. Brain Res. 11*, 335−343.
19. Jakes, R., Spillantini, M. G., and Goedert, M. (1994) *FEBS Lett. 345*, 27−32.
20. George, J. M., Jin, H., Woods, W. S., and Clayton, D. F. (1995) *Neuron 15*, 361−72.
21. Iwai, A., Masliah, E., Yoshimoto, M., Ge, N., Flanagan, L., de Silva, H. A., Kittel, A., and Saitoh, T. (1995) *Neuron 14*, 467−75.
22. Shibayama-Imazu, T., Okahashi, I., Omata, K., Nakajo, S., Ochiai, H., Nakai, Y., Hama, T., Nakamura, Y., and Nakaya, K. (1993) *Brain Res. 622*, 17−25.
23. Withers, G. S., George, J. M., Banker, G. A., and Clayton, D. F. (1997) *Dev. Brain Res. 99*, 87−94.
24. Jenco, J. M., Rawlingson, A., Daniels, B., and Morris, A. J. (1998) *Biochemistry 37*, 4901−4909.
25. Han, H., Weinreb, P. H., and Lansbury, P. T. (1995) *Chem. Biol. 2*, 163−9.
26. Crowther, R. A., Jakes, R., Spillantini, M. G., and Goedert, M. (1998) *FEBS Lett. 436*, 309−12.
27. Weinreb, P. H., Zhen, W., Poon, A. W., Conway, K. A., and Lansbury, P. T., Jr. (1996) *Biochemistry 35*, 13709−13715.
28. Davidson, W. S., Jonas, A., Clayton, D. F., and George, J. M. (1998) *J. Biol. Chem. 273*, 9443−9449.
29. Jensen, P. H., Nielsen, M. S., Jakes, R., Dotti, C. G., and Goedert, M. (1998) *J. Biol. Chem. 273*, 26292−4.
30. Conway, K. A., Harper, J. D., and Lansbury, P. T. (1998) *Nat. Med. 4*, 1318−1320.
31. Hashimoto, M., Hsu, L. J., Sisk, A., Xia, Y., Takeda, A., Sundsmo, M., and Masliah, E. (1998) *Brain Res. 799*, 301−6.
32. El-Agnaf, O. M., Jakes, R., Curran, M. D., and Wallace, A. (1998) *FEBS Lett. 440*, 67−70.
33. Giasson, B. I., Uryu, K., Trojanowski, J. Q., and Lee, V. M. Y. (1999) *J. Biol. Chem. 274*, 7619−22.
34. Narhi, L., Wood, S. J., Steavenson, S., Jiang, Y., Wu, G. M., Anafi, D., Kaufman, S. A., Martin, F., Sitney, K., Denis, P., Louis, J. C., Wypych, J., Biere, A. L., and Citron, M. (1999) *J. Biol. Chem. 274*, 9843−6.
35. Harper, J. D., Lieber, C. M., and Lansbury, P. T. (1997) *Chem. Biol. 4*, 951−959.
36. Harper, J. D., Wong, S. S., Lieber, C. M., and Lansbury, P. T., Jr. (1997) *Chem. Biol. 4*, 119−125.
37. Harper, J. D., Wong, S. S., Lieber, C. M., and Lansbury, P. T., Jr. (1999) *Biochemistry 38*, 8972−80.
38. Walsh, D. M., Lomakin, A., Benedek, G. B., Condron, M. M., and Teplow, D. B. (1997) *J. Biol. Chem. 272*, 22364−72.
39. Kelly, J. W., and Lansbury, P. T., Jr. (1994) *Amyloid: Int. J. Exp. Clin. Invest. 1*, 186−205.
40. Lansbury, P. T., Jr. (1992) *Biochem. 31*, 6865−6870.
41. Kocisko, D. A., Raymond, G., Lansbury, P. T., and Caughey, B. (1996) *Biochem. 35*, 13434−13442.
42. Nordstedt, C., Naslund, J., Tjernberg, L. O., Karlstrom, A. R., Thyberg, J., and Terenius, L. (1994) *J. Biol. Chem. 269*, 30773−30776.
43. Langston, J. W., Sastry, S., Chan, P., Forno, L. S., Bolin, L. M., and Di Monte, D. A. (1998) *Exp. Neurol. 154*, 684−90.
44. Iwai, A., Yoshimoto, M., Masliah, E., and Saitoh, T. (1995) *Biochemistry 34*, 10139−45.
45. Hasegawa, K., Yamashita, I., and Namba, K. (1998) *Biophys. J. 74*, 569−575.
46. Iwatsubo, T., Yamaguchi, H., Fujimuro, M., Yokosawa, H., Ihara, Y., Trojanowski, J. Q., and Lee, V. M. (1996) *Am. J. Pathol. 148*, 1517−29.
47. Spillantini, M. G., Crowther, R. A., Jakes, R., Hasegawa, M., and Goedert, M. (1998) *Proc. Natl. Acad. Sci. U.S.A. 95*, 6469−6473.
48. Woody, R. W. (1995) *Methods Enzymol. 246*, 34−71.
49. Walsh, D. M., Hartley, D. M., Kusumoto, Y., Fezoui, Y., Condron, M. M., Lomakin, A., Benedek, G. B., Selkoe, D. J., and Teplow, D. B. (1999) *J. Biol. Chem. 274*, 25945−25952.
50. Adler, A. J., Greenfield, N. J., and Fasman, G. D. (1973) *Methods Enzymol. 27*, 675−735.
51. Conway, K. A., Lee, S.-J., Rochet, J.-C., Ding, T. T., Williamson, R. E., and Lansbury, P. T., Jr. (2000) *Proc. Natl. Acad. Sci. U.S.A., 97*, 571−576.
52. Bandekar, J., and Krimm, S. (1985) *Int. J. Peptide Protein Res. 26*, 407−415.
53. Krimm, S., and Bandekar, J. (1986) in *Advances in Protein Chemistry* (Anfinsen, C., Ed.) pp 183−364.
54. Ladewig, P. (1945) *Nature 156*, 81.
55. Cooper, J. H. (1974) *Lab. Invest. 31*, 232−238.
56. Puchtler, H., Sweat Waldrop, F., and Meloan, S. N. (1983) *Histochem. 77*, 431−45.
57. Elghetany, M. T., and Saleem, A. (1988) *Stain Technol. 63*, 201−12.
58. Klunk, W. E., Jacob, R. F., and Mason, R. P. (1999) *Anal. Biochem. 266*, 66−76.
59. Klunk, W. E., Pettegrew, J. W., and Abraham, D. J. (1989) *J. Histochem. Cytochem. 37*, 1293−1297.
60. Bonifacio, M. J., Sakaki, Y., and Saraiva, M. J. (1996) *Biochim Biophys Acta 1316*, 35−42.
61. Klunk, W. E., Pettegrew, J. W., and Abraham, D. J. (1989) *J. Histochem. Cytochem. 37*, 1273−1281.
62. LeVine, H., III. (1993) *Protein Sci. 2*, 404−410.
63. Naiki, H., Higuchi, K., Hosokawa, M., and Takeda, T. (1989) *Anal. Biochem. 177*, 244−249.
64. Kudva, Y. C., Mueske, C., Butler, P. C., and Eberhardt, N. L. (1998) *Biochem. J. 331*, 809−13.
65. Nandi, P. K. (1998) *Arch. Virol. 143*, 1251−63.
66. Naiki, H., and Nakakuki, K. (1996) *Lab Invest. 74*, 374−83.

67. Friedhoff, P., Schneider, A., Mandelkow, E. M., and Mandelkow, E. (1998) *Biochemistry 37*, 10223−30.
68. Caughey, B., Raymond, G. J., Kocisko, G. J., and Lansbury, P. T., Jr. (1997) *J. Virol. 71*, 4107−4110.
69. Soto, C., and Castano, E. M. (1996) *Biochem. J. 314*, 701−7.
70. Bolton, D. C., McKinley, M. P., and Prusiner, S. B. (1982) *Science 218*, 1309−1311.
71. Prusiner, S. B., McKinley, M. P., Bowman, K. A., Bolton, D. C., Bendheim, P. E., Groth, D. F., and Glenner, G. G. (1983) *Cell 35*, 349−58.
72. Sipe, J. D. (1992) *Annu. Rev. Biochem. 61*, 947−975.
73. Glenner, G. G., Eanes, E. D., and Page, D. L. (1972) *J. Histochem, Cytochem, 20*, 821−6.
74. Burke, M. J., and Rougvie, M. A. (1972) *Biochemistry 11*, 2435−9.
75. Harper, J. D., and Lansbury, P. T. (1997) *Annu. Rev. Biochem. 66*, 385−407.
76. Goedert, M., Crowther, R. A., and Spillantini, M. G. (1998) *Neuron 21*, 955−8.
77. Friedhoff, P., von Bergen, M., Mandelkow, E. M., Davies, P., and Mandelkow, E. (1998) *Proc. Natl. Acad. Sci. U.S.A. 95*, 15712−15717.
78. Herzfeld, J. (1996) *Acc. Chem. Res. 29*, 31−37.
79. Scherzinger, E., Sittler, A., Schweiger, K., Heiser, V., Lurz, R., Hasenbank, R., Bates, G. P., Lehrach, H., and Wanker, E. E. (1999) *Proc. Natl. Acad. Sci. U.S.A. 96*, 4604−9.
80. Saudou, F., Finkbeiner, S., Devys, D., and Greenberg, M. E. (1998) *Cell 95*, 55−66.
81. Klement, I. A., Skinner, P. J., Kaytor, M. D., Yi, H., Hersch, S. M., Clark, H. B., Zoghbi, H. Y., and Orr, H. T. (1998) *Cell 95*, 41−53.
82. Lansbury, P. T. (1999) *Proc. Natl. Acad. Sci. U.S.A. 96*, 3342−2244.

BI991447R